

Frequency-dependent, dynamic sensing properties of polycrystalline Galfenol ($\text{Fe}_{81.6}\text{Ga}_{18.4}$)

Justin J. Scheidler,^{1,a)} Vivake M. Asnani,² and Marcelo J. Dapino³

¹Universities Space Research Association, NASA Glenn Research Center, Materials and Structures Division, Rotating and Drive Systems Branch, Cleveland, Ohio 44135, USA

²NASA Glenn Research Center, Materials and Structures Division, Rotating and Drive Systems Branch, Cleveland, Ohio 44135, USA

³Department of Mechanical and Aerospace Engineering, The Ohio State University, Columbus, Ohio 43210, USA

(Received 5 April 2016; accepted 8 June 2016; published online 28 June 2016)

This paper presents the first measurement of Galfenol's frequency-dependent strain and magnetic flux density responses to controlled dynamic stress, from which frequency-dependent, effective material properties relating these quantities are calculated. Solid and laminated Galfenol ($\text{Fe}_{81.6}\text{Ga}_{18.4}$) rods were excited by 2.88 MPa compressive stresses up to 1 kHz under constant field and constant current conditions. Due to magnetic diffusion cut-off frequencies of only 59.3 to 145.7 Hz, the dynamic properties of the solid rod are found to vary significantly; this illustrates the inaccuracy of frequency-independent dynamic properties calculated via linear piezomagnetic models from experimental responses to electrical excitation. Conversely, the sensing properties of the laminated rod exhibit a weak dependence on frequency over the measurement range (i.e., a cut-off >1 kHz). The data are used to validate an existing model for mechanically induced magnetic diffusion. Loss factors and magnetomechanical energy densities are also presented and discussed in terms of loss separation, magnetic diffusion, and energy conservation. *Published by AIP Publishing.*

[<http://dx.doi.org/10.1063/1.4954320>]

I. INTRODUCTION

Magnetostrictive materials exhibit bidirectional coupling between their mechanical and magnetic states. Magnetostrictive iron-gallium alloys (Galfenol) exhibit a unique combination of active properties, mechanical strength, and thermal tolerance,¹ which allow for the development of active, load-bearing devices for harsh environments.² A key technical challenge is the very limited experimental data on Galfenol's frequency-dependent response to dynamic stress, which is critically important for the design of such devices and the validation of rate-dependent constitutive models.³ Galfenol's magnetization response to dynamic stress⁴ and its damping capacity⁵ have been reported, but the forcing frequency was limited to 10 Hz in both studies. The Young's modulus, coupling coefficient, and damping ratio of Galfenol rods have been calculated from electrical responses to controlled dynamic currents;⁶ however, this electrically controlled method relies on a linear piezomagnetic model relating electrical and mechanical domains. Besides the potential inaccuracy of linear models, this method cannot quantify the frequency dependence of material properties. This paper reports the first measurement of Galfenol's frequency-dependent strain and magnetic flux density responses to controlled dynamic stress. Dynamic material properties, which are effectively complex-valued and frequency dependent due to stress-induced eddy currents,⁷ were directly calculated from the mechanically excited responses.

II. EXPERIMENTAL SETUP

Solid and laminated rods of $\langle 100 \rangle$ oriented, polycrystalline, research-grade $\text{Fe}_{81.6}\text{Ga}_{18.4}$ were axially excited by a dynamic load frame with a nearly sinusoidal compressive stress having a nominal amplitude of 2.88 MPa and frequency up to 1 kHz; relative to the desired stress sinusoid, the (unwanted) 2nd and 3rd harmonics of the sinusoid had magnitudes of <4% and <3.5%, respectively. A custom magnetic circuit was used to establish a desired magnetic state over a gauge region of the specimens.⁸ The specimens were 7.62 cm long, 0.627 cm diameter rods tolerated according to ASTM standards and designed to prevent buckling.⁸ Using an analytical solution of mechanically induced magnetic diffusion in solid, cylindrical magnetoelastic materials,⁷ the laminate geometry (0.838 mm thick laminates) was selected to balance an increase in the magnetic diffusion cut-off frequency with a reduction in the volume fraction of Galfenol.⁸ Fig. 1 depicts the geometry of the specimens and a cross-section of the laminated specimen, which has 7 full-sized laminates and 1 partial laminate. The specimens were cut from the same bulk rod.

Measured quantities include the axial component of surface strain S , average magnetic flux density B , surface magnetic field H , and the controlled average stress T ; S , B , and H were measured within the gauge region. The specimen's temperature and the current I and voltage V applied to the electromagnets were also measured. An uncertainty analysis and calibration of each sensor were conducted, as detailed previously.⁸ For the laminated specimen, the calibration factor of the magnetic flux density sensing coil was corrected to account for the presence of adhesive layers.

^{a)}justin.j.scheidler@nasa.gov

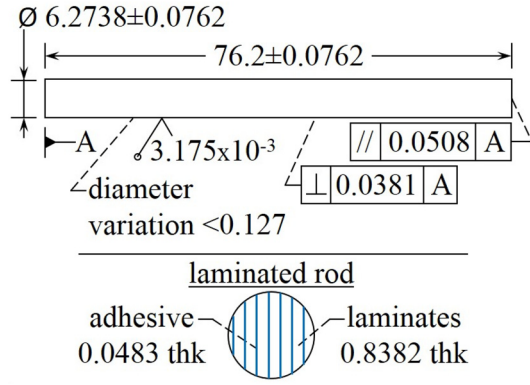
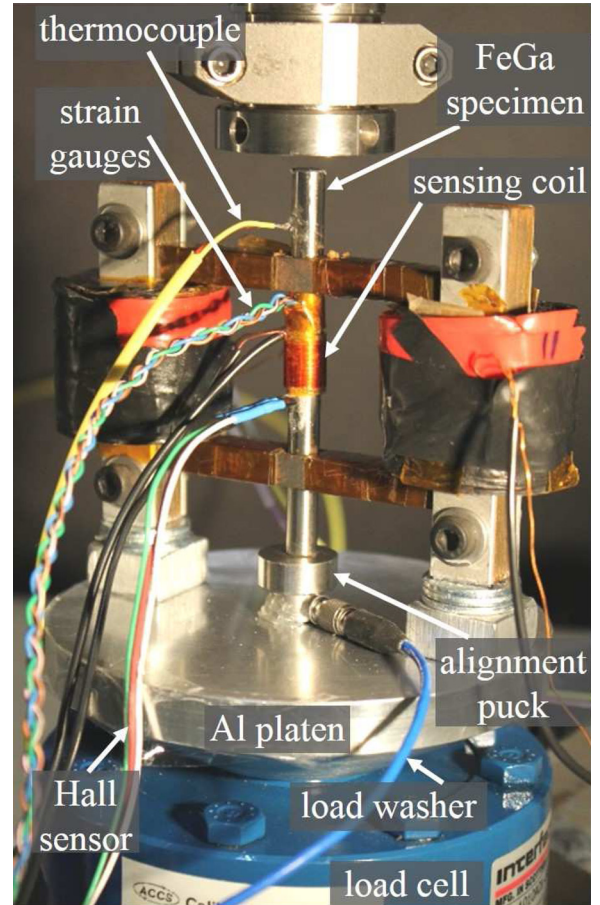


FIG. 1. Specimen geometry and tolerances (dimensions in mm).

Three key sources of error were accounted for: (a) electromagnetic noise in strain signals due to Galfenol's time-varying B , (b) error in force signals due to the inertial force of mechanical fixtures, and (c) phase misalignment between signals due to conditioning electronics, which can significantly affect hysteresis measurements at high frequency.⁸ Electromagnetically induced strain error was kept below 0.74% of the strain span by wiring two collocated strain gauges in series (noise cancellation) and through leadwire weaving. Inertial force error was kept below 0.41% of the loading span by measuring dynamic forces above 100 Hz using a piezoelectric load washer nearly collocated with the specimen. Dynamic forces at frequencies lower than 100 Hz were measured using a load cell. The sensor signals' phase misalignment versus frequency was explicitly measured and then corrected in post-processing.⁸ The experimental setup is shown in Fig. 2.

Strain and magnetic flux density responses to dynamic stress were measured under constant current and constant field at the respective bias states for which the quasi-static, minor loop sensitivity of the *solid* rod was maximized: -9.93 MPa, 0.3 A and -7.96 MPa, 2.46 kA/m.⁸ This is the ideal operating point for many applications. Constant field conditions eliminate the influence of the magnetizing circuit on the constitutive response. However, constant current conditions are easier to achieve in practice, particularly in applications involving high-frequency dynamic stress. During constant current testing, the unintended current variation was ± 1.5 mA, whereas variation in the (uncontrolled) surface field was ± 0.25 kA/m. During constant field testing, the unintended surface field variation was ± 0.05 kA/m up to 100 Hz and about ± 0.23 kA/m from 100 Hz to 1 kHz; due to this degradation in field control, the constant field data ≥ 100 Hz is unreliable. Throughout testing, temperature increases above the 23°C ambient were $< 5^\circ\text{C}$.

The material properties of magnetostrictive materials for axial sensing of stress inputs are the piezomagnetic coefficient $d_{33}^{*H} := \partial B / \partial T^H$ and the Young's modulus $E^H = 1 / s_{33}^H := 1 / (\partial S / \partial T^H)$, where the superscript H signifies measurement under constant field. Properties under constant current are denoted by a superscript I . Herein, the subscript 33 is omitted to simplify the notation. The dynamic sensing properties and energy losses were calculated from the measured constitutive response using a frequency-domain method adapted

FIG. 2. Experimental setup.⁸

from ASTM D5992,⁹ which is illustrated for the constant current condition. After extracting the complex-valued, fundamental component of each signal (e.g., \tilde{T}_1) from Fourier-transformed signals, the dynamic piezomagnetic coefficient and Young's modulus respectively are

$$\tilde{d}^{*I} = \tilde{B}_1 / \tilde{T}_1 = d^{*I} (1 - j\eta_{d^*}^I), \quad (1)$$

$$\tilde{E}^I = \tilde{T}_1 / \tilde{S}_1 = E^I (1 + j\eta_E^I), \quad (2)$$

where d^{*I} and E^I are the lossless components and $\eta_{d^*}^I$ and η_E^I are the associated loss factors that quantify the B - T and S - T hysteresis, respectively. The use of this method is valid because, for the applied excitation, the response was nearly linear, and the sensing properties were essentially constant at each forcing frequency. For the laminated rod, this method gives an effective Young's modulus, because the calculation uses the total stress in the rod, rather than the stress in the laminates. Loss factors are computed as shown in (2) and (1). However, for a linear response, (2) is equivalent to the mechanical loss factor η_{mech} ¹⁰

$$\eta_{\text{mech}} := \frac{W_{\text{d,mech}} / 2\pi}{W_{\text{osc,mech}}} = \frac{(AL \cdot \oint T dS) / 2\pi}{AL \cdot \frac{1}{2} E |\tilde{S}_1|^2}, \quad (3)$$

where $W_{\text{d,mech}}$ is the mechanical energy dissipated by the specimen per cycle, $W_{\text{osc,mech}}$ is the steady-state oscillation

energy stored by the specimen. $W_{\text{osc,mech}}$ is taken as the stored mechanical energy at maximum deflection in a lossless, linear spring of stiffness AE/L , where A and L are the cross-sectional area and length of the rod, respectively.¹⁰

III. MEASUREMENTS

A. Quasi-static response

The response of the specimens to quasi-static compressive stress was measured to verify the experimental setup with existing data, as detailed previously.⁸ The quasi-static (1 Hz) major loop strain response of each specimen at the selected magnetic biases is shown in Fig. 3; the corresponding 4 Hz dynamic minor loop is overlaid on each curve to indicate the bias at which the dynamic measurements were taken. As shown in prior work,^{11,12} within the burst region of each response, the response of a solid rod under constant field is significantly more sensitive to stress than that under constant current. Compared to the solid specimen, the laminated specimen has a lower saturation Young's modulus (59.6 GPa compared to 72.1 GPa), lower magnetic hysteresis, and weaker magnetomechanical coupling at this bias current. These differences can be attributed to fundamental differences in the microstructure and texture of the specimens. For reference, the quasi-static (0.1 Hz) major loop actuation response of the solid specimen was also measured and is depicted in Fig. 4. The saturation magnetostriction is 237×10^{-6} m/m.

B. Dynamic sensing properties

The frequency dependence of the dynamic sensing properties of the solid and laminated Galfenol rods is shown in Figs. 5 and 6; due to inadequate field control, constant field data ≥ 100 Hz is grayed out and disconnected and all references to "data" refer to the trustworthy data points. At low frequency, there is a distinct difference between the sensing properties of the solid and laminated specimens, as observed in quasi-static sensing measurements. The solid rod exhibits a strong

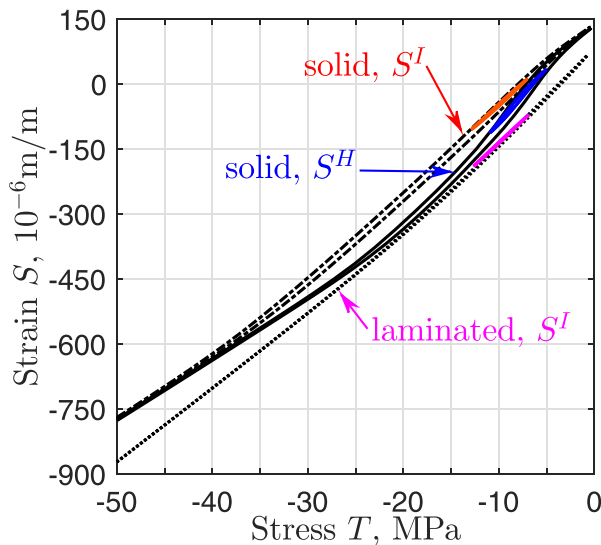


FIG. 3. Quasi-static (1 Hz) major loop strain versus stress response of each specimen measured at constant current (0.3 A) and constant field (2.41 kA/m), overlaid with the corresponding 4 Hz dynamic minor loop.

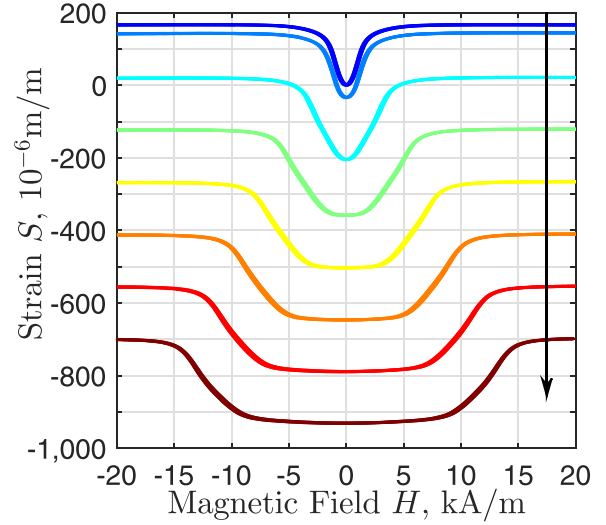


FIG. 4. Quasi-static strain versus magnetic field response of the solid specimen measured at constant stresses of 0.00, -1.64 , -10.23 , -20.44 , -30.65 , -40.88 , -51.10 , and -61.31 MPa; the direction of the arrow denotes increasing bias compression.

dependence on forcing frequency due to eddy currents, which damp domain wall motion, causing the piezomagnetic coefficient to decay toward 0 and the Young's modulus to monotonically approach its saturation value (72.1 GPa). For the specimen geometry, bias states, and frequency range considered, eddy currents dominate the frequency-dependent energy loss in the solid rod. Consequently, the experimental cut-off

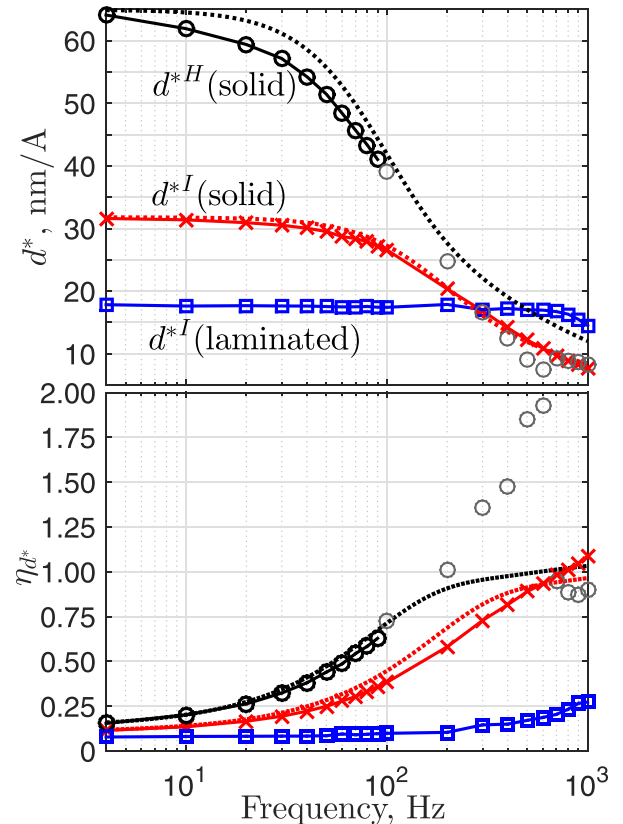


FIG. 5. Dynamic piezomagnetic coefficient measured at constant current (0.3 A) and constant field (2.41 kA/m), lossless component (top) and loss factor (bottom); data (solid), model (dotted).

frequency is defined as the theoretical mechanically induced magnetic diffusion cut-off frequency⁷ (i.e., the frequency when $|\tilde{d}^*|$ (or d^*) has decayed to 82.8% (or 74.8%) of its static value). From Fig. 5, the experimental cut-offs are about 59.3 Hz and 145.7 Hz for constant field and constant current conditions, respectively; the static values were found by extrapolating the data to 0 Hz. This behavior illustrates the need for frequency-dependent measurements and the inaccuracy, even for linear operating regimes, of dynamic properties⁶ calculated via linear piezomagnetic models from experimental responses to electrical excitation. Figs. 5 and 6 also compare the measured data for the solid rod to an existing, linear model⁷ that includes the effect of mechanically induced eddy currents on the dynamic material properties. The model was evaluated using an approximate electrical conductivity¹³ ($\sigma \approx 2.15 \times 10^6$ S/m), magnetic permeabilities estimated from measurements⁸ (constant field: $\mu \approx 350\mu_0$, constant current: $\mu \approx 175\mu_0$), and static values of \tilde{d}^* and \tilde{E} , which were determined by extrapolating the data to 0 Hz. The model closely fits the data through the cut-off frequency despite the use of some estimated properties and imperfect bias and stress control. Above a few hundred Hz, the model deviates from the data, suggesting that other loss mechanisms (e.g., eddy currents in the magnetizing circuit) may become significant; the predicted decrease in η_E above the cut-off should be studied in future work.

The dynamic sensing properties of the laminated rod display a weak dependence on frequency up to 1 kHz. In particular, the experimental cut-off is >1 kHz (extrapolation of the data suggests a cut-off of about 1.2 kHz) and the theoretical cut-off is about 9.5 kHz when a permeability of $175\mu_0$ is used along with an effective conductivity¹⁴ ($\sigma/(7+1)^2$) that approximates the laminated rod as a solid rod. Due to the unavailability of similar measurements, additional testing is needed to determine if this discrepancy is caused by an inaccurate prediction (e.g., due to an incorrect estimate of the permeability or effective conductivity) or if the laminated rod has a unique behavior. It is emphasized that E^I of the laminated rod appreciably decreases between 100 and 300 Hz. Over this frequency range, d_{33}^{*I} is nearly constant, which suggests that the magnetomechanical behavior is not the cause. The root cause is currently unexplained. Similar behavior has been observed below the cut-off frequency of a solid Terfenol-D rod.¹⁵

C. Energy dissipation and conservation

To more closely compare the solid and laminated rods, energy dissipation in the Galfenol rods was also calculated from the constant current data. The energy dissipated per cycle is highly dependent on stress amplitude; thus, it is useful to consider a normalized energy loss, such as the mechanical loss factor, which is equal to η_E in Fig. 6 as mentioned above. Below the cut-off frequency, the solid rod exhibits a nearly linear increase in loss factor with frequency, suggesting that excess eddy current losses are low and there is a high density of magnetic domain walls.¹⁶ This is supported by magnetic domain observations in single crystals of similar Galfenol alloys,¹⁷ which show that magnetic domains are

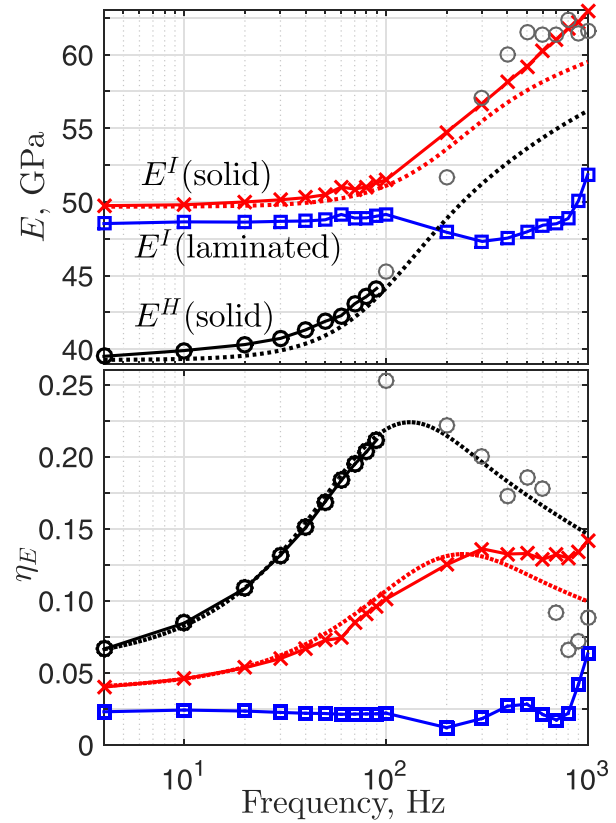


FIG. 6. Dynamic Young's modulus measured at constant current (0.3 A) and constant field (2.41 kA/m), lossless component (top) and loss factor (bottom); data (solid), model (dotted).

about $100 \mu\text{m}$ wide (about 10^2 times smaller than the specimen's diameter). As frequency increases above the cut-off, domain wall motion is significantly suppressed and the loss factor of the solid rod levels off. The loss factor of the laminated rod displays a moderately flat response up to 800 Hz. At high frequency, the loss factor of the solid and laminated rods increase due to viscoelastic material damping, losses in the magnetizing circuit, and, in the laminated rod, the finite laminate thickness (i.e., eddy currents).

To further investigate the magnetomechanical energy loss under constant current, Fig. 7 presents the frequency dependence of the energy density components during steady-state oscillation: (1) mechanical, $\oint T dS$, (2) magnetic (based on the surface field), $\oint H dB$, (3) magnetic (based on an approximate average internal field), $\oint H_{\text{avg}} dB$, and (4) mechanical plus magnetic, $\oint T dS + \oint H_{\text{avg}} dB$. The energy densities per cycle were calculated from the fundamental component of each signal.⁹ H_{avg} is calculated from the measured T and H using the aforementioned magnetic permeabilities and conductivities as discussed by Scheidler and Dapino.⁷ As expected for a mechanical-to-magnetic energy conversion, $\oint T dS > 0$ (mechanical energy is supplied) and $\oint H dB < 0$ (magnetic energy is dissipated/produced).¹⁸ As frequency increases in the solid rod, H_{avg} quickly deviates from H due to magnetic diffusion; consequently, $\oint H dB$ under-predicts the true magnetic energy loss, even at low frequencies. Conversely, in the laminated rod, the magnetic energy can be accurately calculated using a surface field measurement,

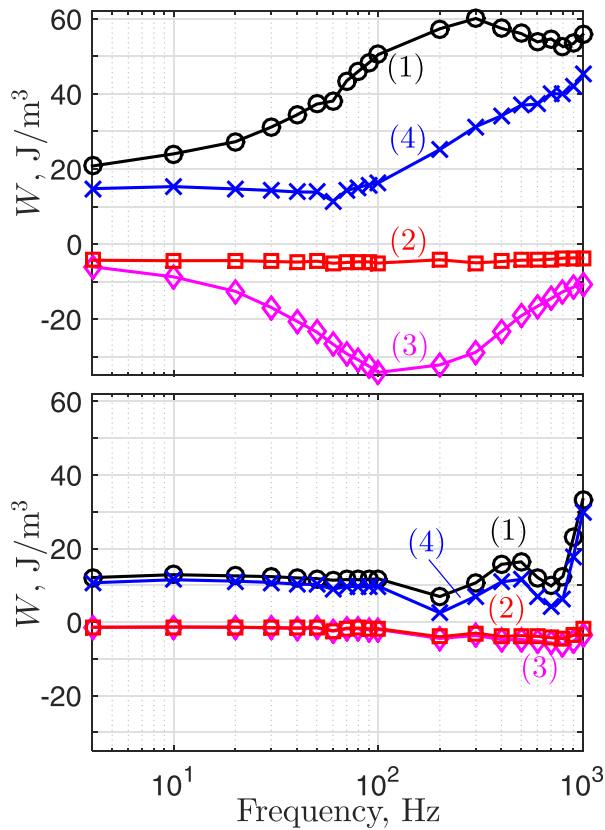


FIG. 7. (1) Mechanical (\circ), (2) magnetic (\square), (3) magnetic (with correction) (\diamond), and (4) loss (corrected) (\times) energy densities per cycle associated with the minor hysteresis loops of the solid (top) and laminated (bottom) $\text{Fe}_{81.6}\text{Ga}_{18.4}$ rods under constant current.

because $H_{\text{avg}} \approx H$ below 1 kHz. The mechanical energy supplied to the rods per cycle is considerably larger than the magnetic energy dissipated in them; this suggests that loss mechanisms other than internal magnetic hysteresis and eddy currents are present. The difference can be accounted for only in part by dissipation to the amplifier, which was measured to be $<10\%$ of the mechanical energy supplied to the solid rod, and viscoelastic damping, which is expected to be small like in other metallic materials. The primary cause may be magnetic hysteresis and eddy currents in the magnetizing circuit; however, this was not studied.

IV. CONCLUSIONS

In summary, the frequency dependence of the dynamic sensing properties of solid and laminated Galfenol ($\text{Fe}_{81.6}\text{Ga}_{18.4}$) rods was explicitly measured under constant current and constant field for 2.88 MPa compressive stresses up to 1 kHz at the bias states for which the quasi-static magnetomechanical coupling of the solid rod was maximized. Due to mechanically induced magnetic diffusion cut-off frequencies of only about 59.3 Hz (constant field) and 145.7 Hz

(constant current), the dynamic sensing properties of the solid rod vary significantly with frequency; the lossless components monotonically trend toward their saturated (passive) values. This result illustrates the inaccuracy of frequency-independent dynamic properties calculated via the dynamic method and also motivates the use of complex-valued, frequency-dependent properties for modeling and design. Conversely, the sensing properties of the laminated rod exhibit a cut-off frequency >1 kHz. The data was used to validate an existing magnetic diffusion model. The close agreement and nearly linear increase in loss factor below the cut-off suggest that excess eddy current losses are low. The frequency dependence of magnetic and mechanical energy densities were also presented and discussed in terms of loss separation, magnetic diffusion, and energy conservation.

ACKNOWLEDGMENTS

This work was supported by the NASA Aeronautics Scholarship Program (Grant No. NNX14AE24H). Additional support was provided by NASA's Revolutionary Vertical Lift Technology project, the NASA Aeronautics Research Mission Directorate Seedling Fund, and the member organizations of the Smart Vehicle Concepts Center, a National Science Foundation Industry/University Cooperative Research Center.

- ¹J. Atulasimha and A. Flatau, *Smart Mater. Struct.* **20**, 043001 (2011).
- ²R. Myers, R. A. Islam, M. Karmarkar, and S. Priya, *Appl. Phys. Lett.* **91**, 122904 (2007).
- ³P. Weetman and G. Akhras, *Appl. Phys. Lett.* **95**, 072504 (2009).
- ⁴L. Weng, B. Wang, M. Dapino, Y. Sun, L. Wang, and B. Cui, *J. Appl. Phys.* **113**, 17A917 (2013).
- ⁵M. Ishimoto, H. Numakura, and M. Wuttig, *Mat. Sci. Eng. A* **442**, 195 (2006).
- ⁶L. M. Twarek and A. B. Flatau, *Proc. SPIE* **5761**, 209–220 (2005).
- ⁷J. Scheidler and M. Dapino, *J. Magn. Magn. Mater.* **397**, 233 (2016).
- ⁸J. J. Scheidler, V. M. Asnani, and M. J. Dapino, "Dynamic characterization of Galfenol ($\text{Fe}_{81.6}\text{Ga}_{18.4}$)," Report No. NASA/TP-2016-218754 (2016).
- ⁹ASTM D5992-96, *Standard Guide for Dynamic Testing of Vulcanized Rubber and Rubber-like Materials Using Vibratory Methods* (ASTM International, West Conshohocken, PA, 2011).
- ¹⁰E. E. Ungar and E. M. Kerwin, Jr., *J. Acoust. Soc. Am.* **34**, 954 (1962).
- ¹¹J. Restorff, M. Wun-Fogle, and E. Summers, *J. Appl. Phys.* **109**, 07A922 (2011).
- ¹²L. Weng, T. Walker, Z. Deng, M. Dapino, and B. Wang, *J. Appl. Phys.* **113**, 024508 (2013).
- ¹³X. Zhao and D. G. Lord, *J. Appl. Phys.* **99**, 08M703 (2006).
- ¹⁴G. Engdahl and A. Bergqvist, *J. Appl. Phys.* **79**, 4689 (1996).
- ¹⁵V. Asnani, Z. Deng, J. Scheidler, and M. Dapino, *Proc. SPIE* **9801**, 98010R (2016).
- ¹⁶*The Science of Hysteresis: Hysteresis in Materials*, 1st ed., edited by G. Bertotti and I. D. Mayergoyz (Academic Press, Oxford, UK, 2006), Vol. 3, pp. 93–97.
- ¹⁷C. Mudivarthi, S.-M. Na, R. Schaefer, M. Laver, M. Wuttig, and A. B. Flatau, *J. Magn. Magn. Mater.* **322**, 2023 (2010).
- ¹⁸J.-H. Yoo, G. Pelligrini, S. Datta, and A. B. Flatau, *Smart Mater. Struct.* **20**, 075008 (2011).